

## REFERENCES

- [1] J. K. Mills and A. Goldenberg, "Force and position control of manipulators during constrained motion tasks," *IEEE Trans. Robot. Automat.*, vol. 5, pp. 30–46, Feb. 1989.
- [2] R. Carelli and R. Kelly, "An adaptive impedance/force controller for robot manipulators," *IEEE Trans. Automat. Contr.*, vol. 36, pp. 967–971, Aug. 1991.
- [3] G. Campion, B. d'Andrea Novel, and G. Bastin, "Controllability and state feedback stability of nonholonomic mechanical systems," *Adv. Robot. Contr.*, pp. 106–124, 1991.
- [4] C. Y. Su, T. P. Leung, and Q. J. Zhou, "Force/motion control of constrained robots using sliding mode," *IEEE Trans. Automat. Contr.*, vol. 37, pp. 668–672, May 1992.
- [5] B. Yao and M. Tomizuka, "Comparative experiments of robust and adaptive control with new robust adaptive controllers for robot manipulators," in *Proc. IEEE Conf. Decision and Control*, Lake Buena Vista, FL, Dec. 1994, pp. 1290–1295.
- [6] J. Q. Gong and B. Yao, "Adaptive robust control without knowing bounds of parameter variations," in *Proc. 38th IEEE Conf. Decision and Control*, Phoenix, AZ, Dec. 1999, pp. 3334–3339.
- [7] M. T. Grabbe and M. M. Bridges, "Comments on 'Force/motion control of constrained robots using sliding mode'," *IEEE Trans. Automat. Contr.*, vol. 39, p. 179, Jan. 1994.
- [8] S. S. Ge, L. Huang, and T. H. Lee, "Model-based and neural-network-based adaptive control of two robotic arms manipulating an object with relative motion," *Int. J. Syst. Sci.e.*, vol. 32, no. 1, pp. 9–23, 2001.
- [9] B. Yao and M. Tomizuka, "Adaptive control of robot manipulators in constrained motion," in *Proc. Amer. Contr. Conf.*, San Francisco, CA, June 1993, pp. 1128–1132.
- [10] S. Chiaverini, B. Siciliano, and L. Villani, "Force/position regulation of compliant robot manipulators," *IEEE Trans. Automat. Contr.*, vol. 39, pp. 647–652, Mar. 1994.
- [11] I. Kolmanovsky and N. H. McClamroch, "Developments in nonholonomic control problems," *IEEE Contr. Syst. Mag.*, vol. 15, pp. 20–36, June 1995.
- [12] S. S. Ge, Z. Sun, T. H. Lee, and M. W. Spong, "Feedback linearization and stabilization of second order nonholonomic chained systems," *Int. J. Contr.*, vol. 74, no. 14, pp. 1383–1392, 2001.
- [13] S. S. Ge, Z. P. Wang, and T. H. Lee, "Adaptive stabilization of uncertain nonholonomic systems by state and output feedback," *Automatica*, vol. 39, no. 8, pp. 1451–1460, 2003.
- [14] C. Y. Su and Y. Stepanenko, "Robust motion/force control of mechanical systems with classical nonholonomic constraints," *IEEE Trans. Automatic Contr.*, vol. 39, pp. 609–614, Mar. 1994.
- [15] D. Wang, Y. C. Soh, and C. C. Cheah, "Robust motion and force control of constrained manipulators by learning," *Automatica*, vol. 31, no. 2, pp. 257–262, 1995.
- [16] Y. C. Chang and B. S. Chen, "Robust tracking designs for both holonomic and nonholonomic constrained mechanical systems: Adaptive fuzzy approach," *IEEE Trans. Fuzzy Syst.*, vol. 8, pp. 46–66, Jan. 2000.
- [17] B. Yao and M. Tomizuka, "Adaptive control of robot manipulators in constrained motion—Controller design," *Trans. ASME Dyn. Syst., Measur. Contr.*, vol. 117, no. 3, pp. 320–328, 1995.
- [18] E. Paljug, T. Sugar, V. Kumar, and X. Yun, "Some important considerations in force control implementation," in *Proc. IEEE Int. Conf. Robotics and Automation*, Nice, France, May 1995, pp. 1270–1275.
- [19] S. S. Ge, T. H. Lee, and C. J. Harris, *Adaptive Neural Network Control of Robot Manipulators*. River Edge, NJ: World Scientific, 1998.
- [20] A. Bloch, M. Reyhanoglu, and N. McClamroch, "Control and stabilization of nonholonomic dynamic systems," *IEEE Trans. Automat. Contr.*, vol. 37, pp. 1746–1757, Nov. 1992.
- [21] A. Astolfi, "On the stabilization of nonholonomic systems," in *Proc. 33rd IEEE Conf. Decision Control*, Lake Buena Vista, FL, Dec. 1994, pp. 3481–3486.
- [22] C. Samson, "Time-varying feedback stabilization of a nonholonomic wheeled mobile robot," *Int. J. Robot. Res.*, vol. 12, pp. 55–66, 1993.

## An Experimental Study of Planar Impact of a Robot Manipulator

Prabhakar R. Pagilla and Biao Yu

**Abstract**—An experimental study of planar impact of a robot manipulator with a stationary rigid surface is presented. Using the data collected from a series of experiments, this paper investigates the post-impact behavior for different pre-impact conditions such as the configuration of the robot, the angle and the velocity of impact. A better understanding of the post-impact behavior for various pre-impact conditions can lead to improved control strategies during impacts in robotic manipulation. Potential applications of this study include robotic assembly and contact tasks. Further, this study could be seen as a preliminary experimental work on impact of general kinematic chains.

**Index Terms**—Constraint, experiments, impact, robot.

### I. INTRODUCTION

Many robotic applications involve interaction of the robot with its environment. Examples include robotic assembly tasks and surface finishing operations such as deburring, grinding, chamfering, and polishing, etc. In many of these applications, the environment is an object to be manipulated or a work piece to be machined. The contact of a robot with an environment will lead to impact if the robot end effector has a nonzero normal velocity component at the point of contact. Modeling of the robot dynamics during impact has received considerable attention in the mechanics literature [1] as well as the robotics literature [16]. The study of the impact phenomenon is essential for stable operation of the robot during contact tasks. The transition from free motion of the robot, to motion on the constrained surface is generally called the transition phase. In the transition phase, the end effector can bounce on the surface due to impact. An experimental understanding of the manipulator impact phenomena will facilitate an efficient design of a stable controller during the transition phase.

Impact models are used to predict the post-impact behavior based on pre-impact conditions. A number of impact models exist in the literature [1], [3], [6]–[8]. Central to the idea of the impact model is the so called coefficient of restitution. There are three widely used coefficients of restitution: 1) the kinematic coefficient (Newton's coefficient), defined as the ratio of the post-impact to the pre-impact normal velocity; 2) the kinetic coefficient (Poisson's coefficient), defined as the ratio of the post-impact to the pre-impact impulse; and 3) the energetic coefficient, defined as the square-root of the ratio of elastic strain energy released during restitution to the energy absorbed by deformation during compression. Extensive discussions on different coefficients of restitution and their applicability can be found in [4]; it also contains a comprehensive discussion on nonsmooth impact mechanics and robot impact control techniques. Impact minimization using redundant degrees of freedom in robots can be found in [15]. A dimensionless model describing the behavior of robot impact with a surface was developed in [17].

The authors' prior work focused on the modeling and control design for a complete robot task [12]. An uncertainty in the location of

Manuscript received December 10, 2001; revised August 18, 2003. This work was supported in part by the National Science Foundation under Grant CMS-9982071.

P. R. Pagilla is with the School of Mechanical and Aerospace Engineering, Oklahoma State University, Stillwater, OK 74078-5016 USA (e-mail: pagilla@okstate.edu).

B. Yu is with Mathworks Inc., Natick, MA 01702 USA.

Digital Object Identifier 10.1109/TMECH.2004.823888

the constraint surface can cause the end effector to land on the surface with a nonzero normal velocity. Experimental observations of robot impact have indicated that the post-impact robot behavior varies considerably for different pre-impact conditions. Some observed aspects include a jump in the tangential velocity and in some cases reversal of the tangential velocity component at the point of impact. Further, for some pre-impact conditions, the post-impact tangential velocity may increase. These effects are qualitatively reported in [14], but were seldom verified experimentally. The increase in the magnitude of the tangential velocity and its direction reversal can cause severe problems during the transition phase. Design of the controller in the transition phase should take these into account when they occur.

The main goal of the study is to obtain an experimental understanding of the post-impact behavior based on different pre-impact conditions; in particular, the focus is on investigating the post-impact tangential velocity of the manipulator end effector for different pre-impact conditions. The experimental study considers the following pre-impact conditions: configuration of the manipulator (up-elbow and down-elbow), angle of impact, and velocity of impact. The study also is intended to identify which impact conditions are significant for post-impact tangential velocity reversal and jump. Insight from these experiments can facilitate design of better control strategies for the transition phase in robotics. In particular, the study will assist in developing compensation terms in the controller to account for direction reversal and jump in the end-effector tangential velocity at impact. Further, the experimental results are compared with the predictions from an impact model developed for the manipulator dynamics, which is based on the classical rigid body theory with kinematic coefficient of restitution.

The rest of the paper is organized as follows. Section II presents the manipulator impact dynamics and discusses the impact phenomena and its governing equations. Experimental procedure and manipulator configurations are discussed in Section III. A representative sample of the experimental results is discussed in Section IV. Section V gives conclusions of the study and some future research directions.

## II. MANIPULATOR IMPACT DYNAMICS

The main hypothesis for the experimental study is that the post-impact tangential velocity can jump and change direction depending on the pre-impact conditions. To predict post-impact behavior based on pre-impact conditions, the classical rigid body approach with kinematic coefficient of restitution is chosen. Theoretical predictions from this approach are compared with the experimental results.

In general, there are three main approaches to study the impact problem: the classical rigid body approach with restitution coefficients, the compliant model approach, and the differential-like approach introduced by Keller. Keller's approach is in some sense an amalgam of the rigid body and the compliant approaches. The three approaches are discussed in considerable detail in [4]. Since the planar manipulator and the impact surface are very rigid, the classical rigid body approach is chosen for this study; the two links of the planar manipulator are machined out of solid aluminum blocks, and hence are very rigid; also, there are no compliant transmission elements in the manipulator because it is a direct drive manipulator, i.e., the links are directly mounted on the rotor of the motor. Further, the kinematic coefficient of restitution is chosen over the kinetic and energetic coefficients because it gives a closed-form expression for the post-impact tangential velocity as a function of the pre-impact conditions. In the following, governing equations for a planar manipulator subject to impact are developed.

Consider the schematic of a two-degree-of-freedom planar manipulator and a contact surface as shown in Fig. 1. Let the forward kinematic

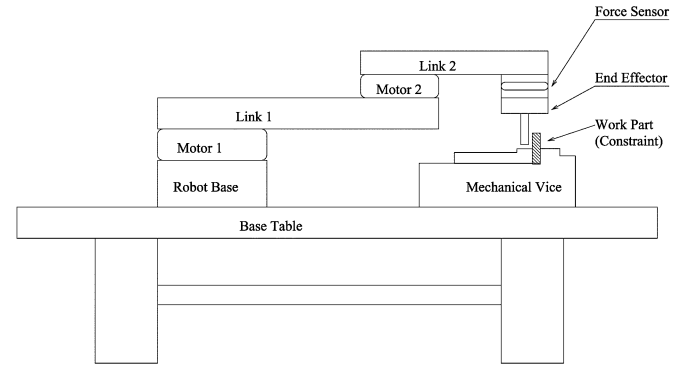


Fig. 1. Planar manipulator and the constraint fixture.

map of the manipulator be  $x = h(q)$ , where  $q \in \mathbb{R}^2$  is the joint position vector and  $x \in \mathbb{R}^2$  is the Cartesian position vector. Then, the velocity kinematics is  $\dot{x}(q) = J(q)\dot{q}$ , where  $J(q)$  is the Jacobian associated with the forward kinematic map. The dynamics of the manipulator is given by

$$M(q)\ddot{q} + C(q, \dot{q})\dot{q} + g(q) = \tau + J^T(q)f \quad (1)$$

where  $M(q)$  is the symmetric positive-definite inertia matrix,  $C(q, \dot{q})$  is the matrix composed of Coriolis and centripetal forces,  $g(q)$  is the gravity vector,  $\tau$  is the vector of joint motor torques,  $f$  is the vector of contact forces. Let the constraint surface be denoted by

$$\phi(x(q)) = 0 \quad (2)$$

where  $\phi: \mathbb{R}^2 \rightarrow \mathbb{R}$ . The state space of the manipulator can be divided into the following:

$$X_u = \{q, \dot{q} \in \mathbb{R}^2 : \phi(q) < 0\} \quad (3)$$

$$X_c = \{q, \dot{q} \in \mathbb{R}^2 : \phi(q) = 0\} \quad (4)$$

$$X_f = \{q, \dot{q} \in \mathbb{R}^2 : \phi(q) > 0\} \quad (5)$$

where  $\phi(q) = \phi(x(q))$  is an abuse of notation, the set  $X_u$  denotes “unconstrained” manipulator configurations away from the surface, the set  $X_c$  denotes configurations in which the manipulator is “constrained” to the surface, and  $X_f$  denotes configurations that are “unreachable” by the manipulator. The gradient of the surface,  $\nabla\phi(q)$ , is always normal to  $\phi$ . Notice that  $\nabla\phi(q)$  points “into” the surface. Therefore, the set  $X_c$  can be further subdivided into two sets  $X_{ct}$  and  $X_{ca}$ , that is,  $X_c = X_{ct} \cup X_{ca}$ , given by

$$X_{ct} = \{q, \dot{q} \in \mathbb{R}^2 : \phi(q) = 0, n \cdot \dot{q} > 0\} \quad (6)$$

$$X_{ca} = \{q, \dot{q} \in \mathbb{R}^2 : \phi(q) = 0, n \cdot \dot{q} = 0\} \quad (7)$$

where  $n := \nabla\phi(q)/\|\nabla\phi(q)\|$  is the unit normal vector to the constraint surface. The condition  $n \cdot \dot{q} > 0$  at contact means that the end effector collides with the surface. Depending on the pre-impact conditions, the end effector may bounce on the surface. It is essential to stabilize the end effector onto the surface before performing a surface finishing operation which involves simultaneous motion and force control of the robot. For a detailed description of dynamic modeling of the robot performing surface finishing operations we refer the reader to [12], [20].

Impacts are generally treated as very large forces acting over a short duration of time. If we assume that the impact occurs over an infinitesimally small period of time, then all velocities remain finite and there is no change in the position of the system. If  $\Delta t \rightarrow 0$  is the duration of collision then the force impulse  $p_I$  due to impact at time  $t_*$  is

$$p_I = \int_{t_*}^{t_* + \Delta t} f(\omega) d\omega \quad (8)$$

where  $f(\cdot)$  is the impact force. Integrating (1) from  $t_*$  to  $t_* + \Delta t$ , the dynamics during impact becomes

$$M(q)\sigma_{\dot{q}} = J^T(q)p_I \quad (9)$$

where  $\sigma_{\dot{q}} := \dot{q}_+ - \dot{q}_-$ , and  $\dot{q}_-$  and  $\dot{q}_+$  denote pre-impact and post-impact velocities, respectively. In the Cartesian coordinates, the change in velocity is given by

$$\sigma_v := H p_I \quad (10)$$

where  $v := \dot{x}$ ,  $\sigma_v := v_+ - v_-$ , and  $H := J(q)M^{-1}(q)J^T(q)$ . One method of obtaining post-impact velocity from pre-impact velocity is to assume Newton's restitution model for normal velocity, that is

$$n^T v_+ = -e_n n^T v_- \quad (11)$$

where  $e_n$  denotes the normal coefficient of restitution. Premultiplying (10) by  $n^T$  and substituting (11) yields

$$-(1 + e_n)n^T v_- = n^T H p_I. \quad (12)$$

Assuming that the contact force impulse is of the form  $p_I = \lambda_n n$ , where  $\lambda_n$  is the magnitude of the normal impulse, (12) can be simplified to

$$\lambda_n = -(1 + e_n) \frac{n^T v_-}{n^T H n}. \quad (13)$$

Let  $t$  be the unit tangential vector to the constraint surface. Premultiplying (10) with  $t^T$  and simplifying we obtain

$$t^T \sigma_v = t^T H n \lambda_n. \quad (14)$$

Substituting (13) into (14) we obtain

$$t^T v_+ = t^T v_- - \frac{t^T H n}{n^T H n} (1 + e_n) n^T v_-. \quad (15)$$

Equations (11) and (15) give the post-impact normal and tangential velocities, respectively. Note that the calculations given by (10) through (15) are standard in the impact literature; they are provided here for completeness. From (15), notice that there is a jump in the tangential velocity given by (15); this jump is primarily due to the configuration of the robot; and the sign of  $t^T H n$  determines the sign of the jump in the tangential velocity.

For a nonideal impact, the contact force impulse,  $p_I$ , generally has components both in the normal and the tangential directions. The contact force impulse can be expressed as  $p_I = \lambda_n n + \lambda_t t$ , where  $\lambda_n$  and  $\lambda_t$  are the magnitudes of the normal force impulse and the tangential force impulse, respectively. To compute  $\lambda_n$ ,  $\lambda_t$ , and the post-impact tangential velocity for the nonideal case, we require another equation in addition to (10) and (11). The additional equation can be obtained by assuming the existence of a kinetic coefficient of restitution [1]. The contact force impulse in the tangential direction for the nonideal case is generally small compared to the normal component when the friction coefficient is small; this assumption is validated by our experimental results, which are discussed in the following sections.

### III. EXPERIMENTAL PLATFORM

The experimental platform consists of a two-axis direct-drive manipulator, which is shown in Fig. 1. Each axis is driven by an NSK Megatorque direct drive servo-motor, which is capable of a maximum velocity of up to three revolutions per second, and has a motor resolver resolution of 156 400 counts per revolution. A force sensor and an end effector are mounted on link 2 as shown in Fig. 1. The end effector consists of a circular plate and a metal probe. For surface finishing operations the circular plate is replaced by a deburring tool and the probe

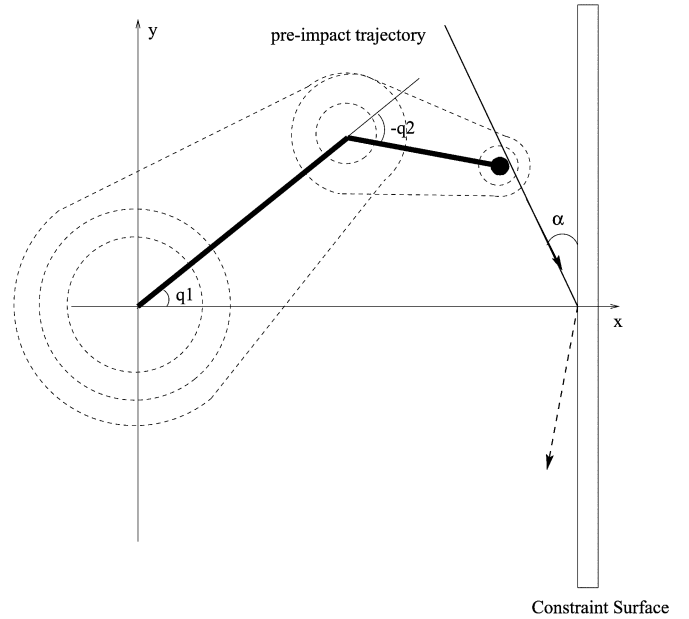


Fig. 2. Up-elbow configuration.

is replaced by a cutting or polishing tool. A mechanical vice firmly holds a thick aluminum piece, which acts as the constraint surface.

#### A. Experimental Procedure

The experimental procedure consists of the manipulator moving toward the surface at a certain impact angle and making contact with the surface; a prescribed velocity of the end effector and the angle of impact is maintained using the motor torques; just prior to impact with the surface the motor torques are shut off to mimic free impact. Joint angles, joint velocities and forces on the end effector are collected every four milli-seconds. Two manipulator configurations, up-elbow and down-elbow, shown in Figs. 2 and 3, respectively, are considered; where  $\alpha$  denotes the angle of impact. For each configuration we consider three velocities of impact (0.1, 0.2, and 0.3 m/s) and four angles of impact (30°, 45°, 60°, and 90°). Impact velocities larger than 0.3 m/s were not considered because the impact force exceeds the force sensor safety limit. A representative sample of the experimental results is shown and discussed in the next section; the reader is referred to [20] for a discussion of all the impact experiments.

### IV. EXPERIMENTAL RESULTS

Experimental results are shown in Figs. 4–10. Figs. 4–7 show data corresponding to the impact velocity of 0.2 m/s and an impact angle of 45°. Figs. 4 and 5 show the time trajectories of the velocity and force, respectively, in the normal and the tangential directions; notice that, for the same impact condition, the impact force and the post-impact velocity are clearly dependent on the configuration of the robot. Further, this is clear from the Cartesian space trajectories of the end effector shown in Figs. 6. Fig. 7 shows a plot of the tangential velocity versus the normal velocity around the impact point; this impact map shows ten samples of data around impact for the up-elbow and the down-elbow configurations; it is clear from this map that the post-impact tangential velocity for the down-elbow configuration reverses direction where as for the up-elbow configuration it does not reverse direction; further, for the up-elbow configuration, the magnitude of the post-impact tangential velocity increases. Therefore, from the experimental results, it can be observed that the post-impact normal velocity does not depend on configuration, which validates (11), but the post-tangential velocity is

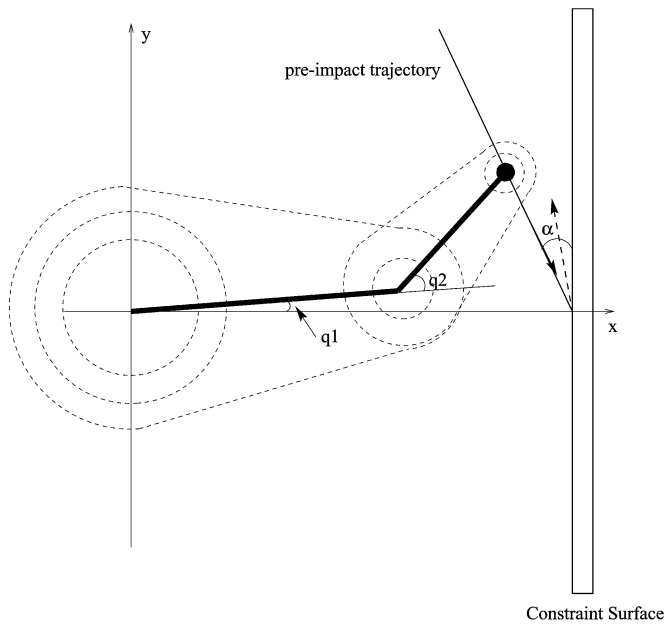


Fig. 3. Down-elbow configuration.

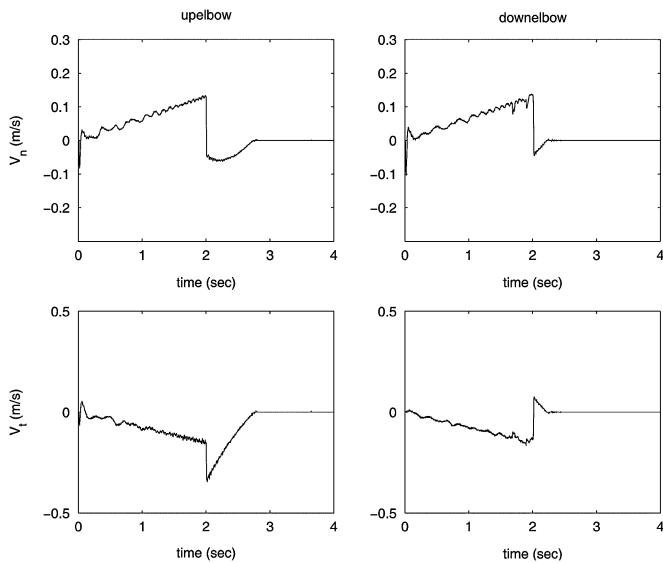


Fig. 4. Normal and tangential velocities for up-elbow and down-elbow configurations. Impact velocity = 0.2 m/s and impact angle = 45°.

a function of the manipulator configuration, which qualitatively validates (15).

Kinetic energy loss due to impact as a function of the impact angles for the up-elbow and the down-elbow configurations and for all three impact velocities is shown in Fig. 8. Notice that the kinetic energy loss depends on the impact velocity, the impact angle, and the configuration. For the same impact angle and manipulator configuration, Fig. 8 shows that the kinetic energy loss is a function of the square of the normal impact velocity; we can also deduce this from (11) and (15).

Table I contains the experimentally computed Newton's and energetic coefficients of restitution for the impact velocity of 0.2 m/s and for different impact angles. Notice that the values are not consistent, especially the values corresponding to the energetic coefficients of restitution. The Newton's coefficient of restitution is calculated using (11) and the experimental data of the pre- and post-impact normal velocity. The experimental energetic coefficient of restitution is defined as the

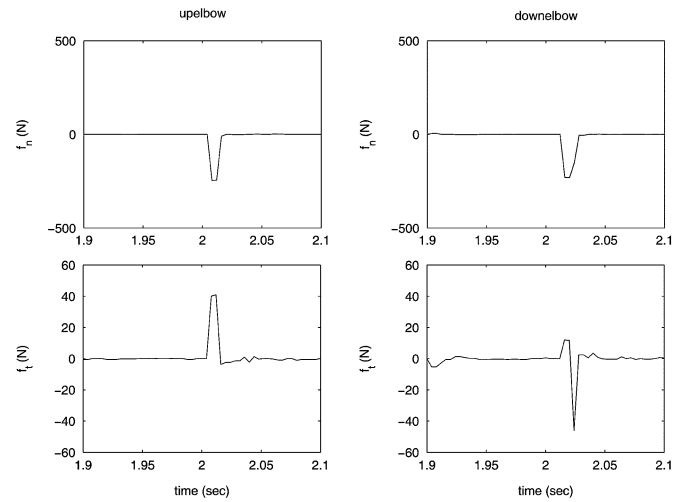


Fig. 5. Normal and tangential forces for up-elbow and down-elbow configurations. Impact velocity = 0.2 m/s and impact angle = 45°.

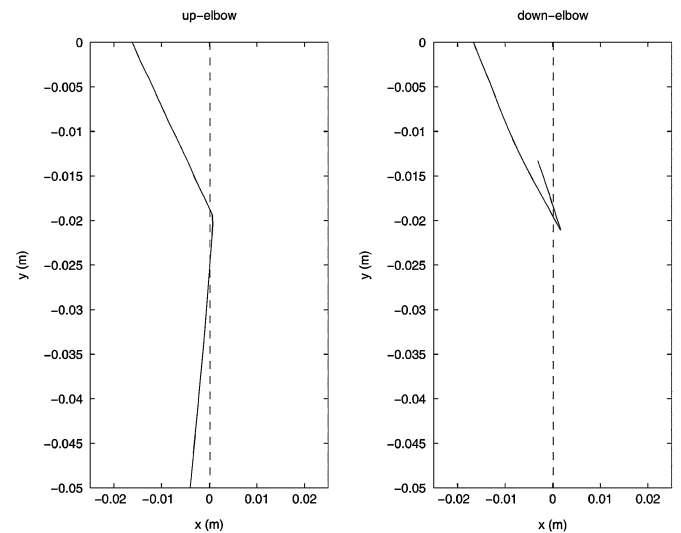


Fig. 6. Manipulator end-effector path in Cartesian space near impact. Impact velocity = 0.2 m/s and impact angle = 45°.

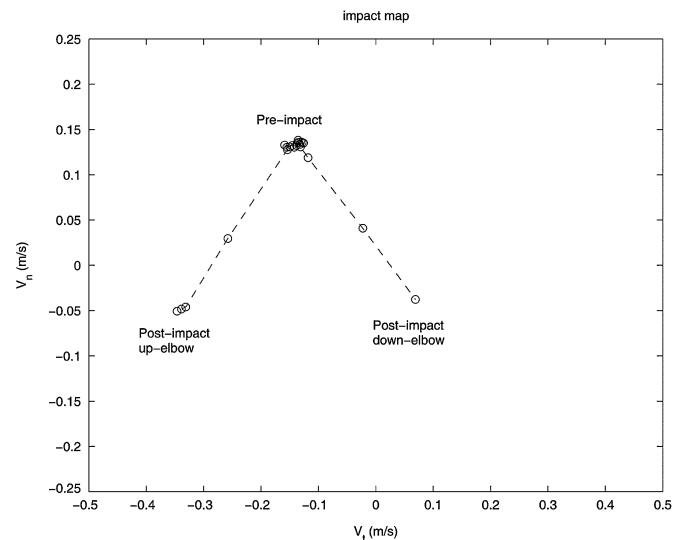


Fig. 7. Impact velocity map. Impact velocity = 0.2 m/s and impact angle = 45°.

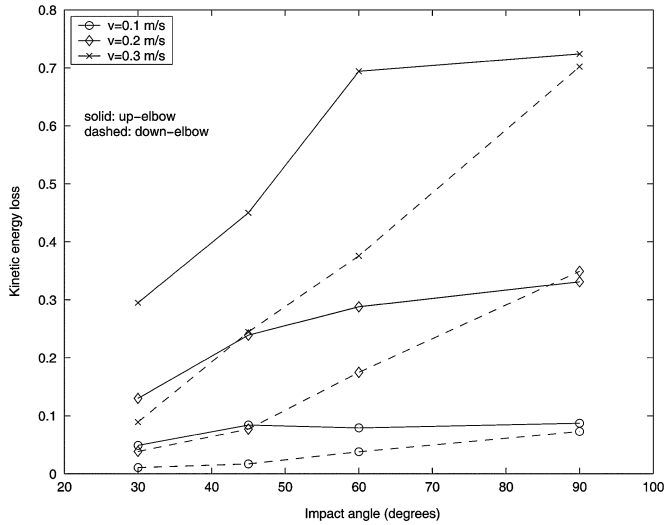


Fig. 8. Kinetic energy loss for up-elbow and down-elbow configurations for three different impact velocities and four different impact angles.

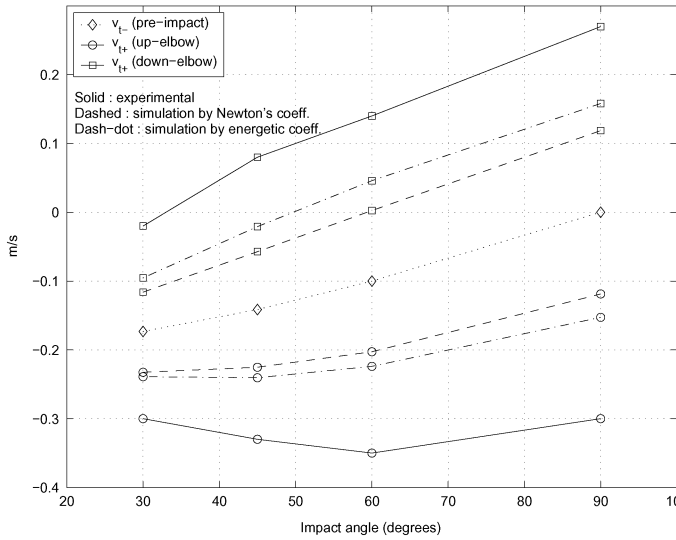


Fig. 9. Pre- and post-impact tangential velocity for up-elbow and down-elbow configurations. Impact velocity = 0.2 m/s. Post-impact tangential velocities for the simulation are obtained by using Newton's and energetic coefficients in (15).

square root of the ratio of the post-impact kinetic energy to the pre-impact kinetic energy and is calculated from the experimental data

$$\text{Energetic coefficient} = \sqrt{\frac{\dot{q}_+^T M(q) \dot{q}_+}{\dot{q}_-^T M(q) \dot{q}_-}}. \quad (16)$$

Figs. 9 and 10 show the post-impact tangential and normal velocities, respectively, for the impact velocity of 0.2 m/s and for different angles of impact and configurations. Fig. 9 shows the experimental data as well as the simulation data obtained from (15). Two sets of simulation data, obtained from (15), is presented; they correspond to the Newton's coefficients of restitution and the experimental energetic coefficients of restitution, which are given in Table I. It can be observed that (15) can predict the change in the direction of the tangential velocity for the down-elbow case even with large variations in the coefficient of restitution; further it can predict the increase in magnitude of the tangential velocity for the up-elbow case. Notice that the experimental results and theoretical predictions seem to match up to a scaling constant. This variation is expected as it is still not clear in the impact literature as to

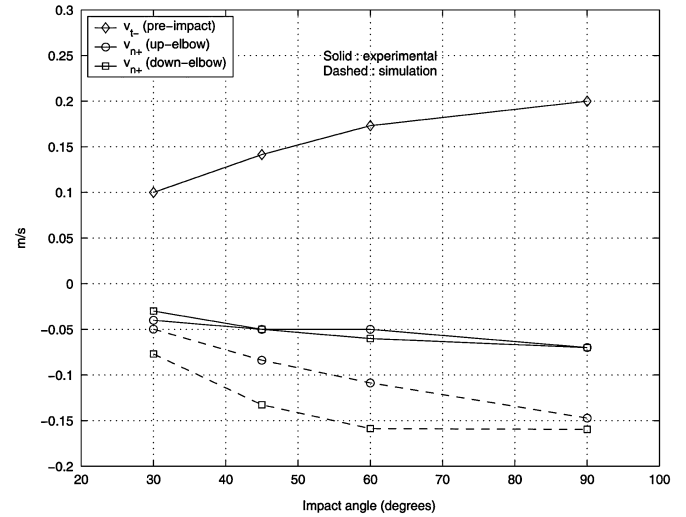


Fig. 10. Pre- and post-impact normal velocity for up-elbow and down-elbow configurations. Impact velocity = 0.2 m/s. Post-impact normal velocity is obtained by using experimentally computed energetic coefficient of restitution in (11).

TABLE I  
COEFFICIENTS OF RESTITUTION

Impact velocity = 0.2 m/s	30°	45°	60°	90°
Newton's down-elbow	0.30	0.35	0.34	0.35
Newton's up-elbow	0.40	0.35	0.28	0.35
Energetic down-elbow	0.76	0.93	0.91	0.79
Energetic up-elbow	0.49	0.59	0.62	0.73

which process parameters influence the value of the kinematic coefficient of restitution.

Therefore, based on the knowledge of the inertia matrix  $H$ , (15) can predict whether the post-impact tangential velocity will reverse direction or increase in magnitude. Hence, the design of better transition controllers to stabilize the tangential velocity of the end effector after impact is feasible because an accurate value of the coefficient of restitution is not required. In [12], a compensation scheme is used in the normal velocity direction after impact in an effort to stabilize the end effector onto the constraint surface. An additional compensation term in the controller to account for the reversal in the tangential velocity, as is done for the normal velocity, may provide stable transition of the end effector onto the constraint surface. A possible strategy is to predict, using (15), the post-impact tangential velocity and then design the additional compensation term in the transition controller to account for either a reversal or increase in magnitude.

## V. CONCLUSION

An experimental study was conducted to investigate the post-impact behavior for various pre-impact conditions. Some key observations from the study are summarized in the following: 1) post-impact tangential velocity can increase in magnitude or reverse direction; this is primarily dependent on the configuration of the manipulator; for the down-elbow configuration, the post-impact tangential velocity either reduces or completely reverses direction; the reversal occurs for higher impact angles; for the up-elbow configuration the magnitude of the post-impact tangential velocity is increased without changing direction; and 2) Comparison of the experimental results with predictions from the classical rigid body impact theory with kinematic coefficient of restitution shows that the theory predicts the general trend observed

in the experimental results; further, the theoretical prediction of the direction reversal of the tangential velocity is not sensitive to the value of the coefficient of restitution.

The study reinforces that the rigid body approach with kinematic coefficient can be conveniently used for closed-form predictions of tangential velocity jumps based on pre-impact conditions for engineering applications. Notice that, since the energetic coefficient given by (16) is not linear in the post- and pre-impact velocities, it is not clear as to how one can obtain a closed-form equation similar to (15) by using the energetic coefficient.

In our previous work [12], we had designed the transition controller with the primary motivation that stable convergence of the end effector onto the surface should be achieved; it was assumed that the tangential velocity component is continuous at the impact. The control goal during the transition phase was to drive the end-effector velocity normal to the surface to zero; that is, only jumps in the normal velocity were considered in designing the compensation terms in the transition controller. This experimental study indicates that discontinuities in both the normal and tangential velocity components must be considered in the transition controller design for better performance. Based on the results of this paper, future work in the design of the transition controller should focus on introducing robustness to discontinuous velocity in both the normal and the tangential directions. To the best of our knowledge, most research in contact transition control literature has not considered the discontinuous behavior of the post-impact tangential velocity.

Although this experimental study is for impact of a planar manipulator with a stationary surface, it can be seen as a preliminary experimental work on impact of general kinematic chains. In practice, there are many kinematic chains with more than two links that experience impacts; this study can be extended to kinematic chains with more than two links. One possible approach is to study a three link manipulator by placing a third link on the two-link planar manipulator used in this study. Also, it is important to investigate the effect of friction between the end effector and the surface; in the presence of friction, the tangential impulse cannot be ignored.

#### ACKNOWLEDGMENT

The authors would like to thank H. Zhong for his help in plotting the experimental data and for conducting some useful computer simulations. The authors also wish to thank the reviewers for providing numerous very useful suggestions for improving the paper.

#### REFERENCES

- [1] R. M. Brach, *Mechanical Impact Dynamics: Rigid Body Collisions*. New York: Wiley, 1991.
- [2] W. Goldsmith, *Impact: The Theory and Physical Behavior of Colliding Solids*. London, U.K.: E. Arnold, 1960.
- [3] V. V. Kozlov and D. V. Treshcev, *Billiards: A genetic introduction to the dynamics of systems with impacts*. Providence, RI: AMS, 1991, vol. 89.
- [4] B. Brogliato, *Nonsmooth Mechanics: Models, Dynamics and Control*, 2nd ed. London, U.K.: Springer-Verlag, 1999.
- [5] D. Stoianovici and Y. Hurmuzlu, "A critical study of the applicability of rigid body collision theory," *ASME J. Appl. Mech.*, vol. 63, pp. 307–316, 1996.
- [6] Y. Hurmuzlu, "An energy-based coefficient of restitution for planar impacts of slender bars with massive external surfaces," *ASME J. Appl. Mech.*, vol. 65, pp. 952–962, 1998.
- [7] C. E. Smith, "Predicting rebounds using rigid body dynamics," *ASME J. Appl. Mech.*, vol. 58, pp. 754–758, 1991.
- [8] W. J. Stronge, "Rigid body collisions with friction," *Proc. R. Soc. Lond. A, Math. Phys. Sci.*, vol. A431, pp. 169–181, 1990.
- [9] —, "Classical planar impact theory and the tip impact of a slender rod," *Int. J. Impact Eng.*, vol. 13, no. 1, pp. 21–33, 1993.

- [10] R. M. Brach, "Predicting rebound using rigid body dynamics," *ASME J. Appl. Mech.*, vol. 59, pp. 700–706, 1992.
- [11] J. B. Keller, "Impact with friction," *ASME J. Appl. Mech.*, vol. 53, pp. 1–4, 1985.
- [12] P. R. Pagilla and B. Yu, "A stable transition controller for constrained robots," *IEEE/ASME Trans. Mechatron.*, vol. 6, pp. 65–74, Mar. 2001.
- [13] —, "An experimental study of planar impact of a robot manipulator," in *IEEE Int. Conf. Robotics and Automation*, Seoul, S. Korea, May 2001.
- [14] C. E. Smith and P. Liu, "Coefficients of restitution," *J. Appl. Mech.*, vol. 59, pp. 963–969, 1992.
- [15] I. D. Walker, "Impact configurations and measures for kinematically redundant and multiple armed robot systems," *IEEE Trans. Robot. Automat.*, vol. 10, pp. 670–683, May 1994.
- [16] R. Volpe and P. Khosla, "A theoretical and experimental investigation of impact control for manipulators," *Int. J. Robot. Res.*, vol. 12, pp. 351–365, 1993.
- [17] K. Youcef-Toumi and D. A. Gutz, "Impact and force control: Modeling and experiments," *ASME J. Dyn. Syst. Measur. Contr.*, vol. 16, pp. 89–98, 1994.
- [18] G. G. Adams, "Imperfectly constrained planar impacts—A coefficient-of-restitution model," *Int. J. Impact Eng.*, vol. 19, no. 8, pp. 693–701, 1997.
- [19] A. Tornambe, "Modeling and control of impact in mechanical systems: Theory and experimental results," *IEEE Trans. Automat. Contr.*, vol. 44, pp. 294–309, Feb. 1999.
- [20] B. Yu, "Modeling, control design, and mechatronic implementation of constrained robots for surface finishing applications," Ph.D. dissertation, School Mech. Aerosp. Eng., Oklahoma State Univ., Stillwater, Dec. 2000.